Astron. Astrophys. 329, 229–232 (1998)

ASTRONOMY
AND
ASTROPHYSICS

Research Note

Chromospheric and coronal activity levels in the nearby faint M dwarf Gl 105B

J.G. Doyle[1], **C.I. Short**[1], **P.B. Byrne**[1], **and P.J. Amado**[1]

Armagh Observatory, College Hill, Armagh BT61 9DG, Northern Ireland, UK

Received 20 May 1997 / Accepted 20 August 1997

Abstract. Monitoring with the HRI onboard ROSAT failed to detect the nearby faint M dwarf star Gl 105B (a star of anomalously low chromospheric and coronal activity), implying $log\ L_x\ <\ 26.1$. High resolution optical data for Ca II HK indicate a surface flux of $\sim$ 6.5 $10^3\ erg\ cm^{-2}\ s^{-1}$, in good agreement with the previously measured Mg II hk flux. Based on chromospheric modelling, both the Hα and Ca II K line profiles indicate an atmospheric structure which is intermediate between that of an intermediate dM chromosphere and a basal chromosphere. Also, the modelling indicates that a better fit is obtained using a model atmosphere which has $T_{\rm min}$ less than 2650 K, and a thin, steep chromosphere. Furthermore, the Ca II HK radiative losses may only be $\sim$5% of the radiative losses in the UV continuum, implying total chromospheric losses in excess of $10^5\ erg\ cm^{-2}\ s^{-1}$.

Key words: stars: Gl 105B; activity; chromospheres; late-type

1. Introduction

For many years, it has been considered that the heating of cool star chromospheres is dominated by magnetic field related mechanisms. This view is based on the observational result that for most stars the chromospheric emission flux is correlated with stellar rotation, which in turn is correlated with the magnetic flux at the stellar surface. However, an alternate mechanism for heating a chromosphere is acoustic wave energy, produced in abundance by convection (Ulmschneider, 1991). Although late-type stars in general show rates of chromospheric heating which are believed to be too high for acoustic heating, exceptions to this have been noted. In recent work, Mathioudakis & Doyle (1992) and Byrne (1993) report a rare population of late-type dwarfs whose chromospheric emission is many orders of magnitude less than that of the Sun. One of the weakest chromospheric stars yet found is the nearby M dwarf, Gl 105B (Byrne, 1993). Gl 105B (=LHS 16) is classified as a dM3.5 star by Henry et al. (1994) and from the photometric colors has an effective temperature of 3200K (Leggett 1992). It's chromospheric Mg II emission is almost two orders of magnitude weaker than the Sun!

A critical test of the nature of this star would be a deep X-ray exposure to attempt the detection of its coronal emission. Unfortunately, at a distance of 7.7 pc (Henry et al. 1994), it was outside the limiting distance of 6 pc for the ROSAT PSPC survey carried out by Schmitt et al. (1995). In this paper we report a long X-ray exposure taken with the High Resolution Imager onboard ROSAT, plus high resolution spectra in order to resolve the Ca II HK lines plus Hα.

Send offprint requests to: J.G. Doyle

2. Observational data

2.1. The optical spectra and their reduction

High-resolution spectroscopic observations of Gl 105B were obtained during part of a 4-night observing run in July/August 1993 carried out with the Utrecht Échelle Spectrograph (Unger & Pettini 1993) on the William Herschel 4.2-meter Telescope (WHT) on La Palma. The dispersed light was recorded on an EEV6 CCD detector with a pixel size of 22.5μm and dimensions of 1280 $\times$ 1180 pixels. The grating used give a resolving power R $\sim$45,000. Four integrations of 30 min. each were taken in the blue, while a single 30 min integration covering Hα was obtained.

CCD reduction, spectrum extraction and calibration were performed with IRAF. After bias subtraction and flat-fielding, only the spectral apertures for Ca II HK and Hα were defined by reference to the flat-field images and the object spectrum extracted. Th-Ar arc exposures were used for the wavelength calibration. A rms error of $\sim$0.005Å was found. The mean con-

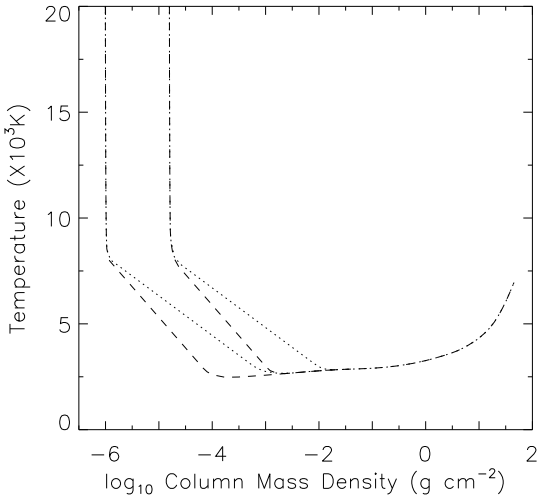

Fig. 1. Temperature structure of models in grid. $1A$ series: dotted lines, $2A$ series: dashed lines.

Table 1. WHT observing run of July/August 1993

Line	FWHM	Observed ($erg\,cm^{-2}\,s^{-1}$)
Ca II K	0.243±0.015	3.96 ± 0.21 10^{-15}
Ca II H	0.224±0.032	2.52 ± 0.28 10^{-15}

tinuum spectrum around Ca II HK typically had S/N 4 per pixel, with a S/N twice this value in the red.

Absolute flux calibration of Ca II HK was by reference to the lower resolution INT data for Gl 105B from Doyle et al. (1994). This paper suggested that the flux calibration is good to 30%. Based on this, the Ca II HK flux at the Earth is 6.5 10^{-15} $erg\ cm^{-2}\ s^{-1}$ (see Table 1), a factor of 3 lower than the upper limit quoted by Doyle et al. (1994).

Using the Gl 105B radius estimate from Mathioudakis & Doyle (1992) implies a surface flux of 6.6 10^3 $erg\,cm^{-2}\,s^{-1}$. The observed Ca II K profile, plus Hα are given in Figs. 2 & 3. Hα is clearly visible as an absorption feature with an EW of 0.2Å. Previous observations (e.g. Stauffer & Hartmann, 1986) indicated a much smaller absorption EW of 0.05Å. The Ca II HK lines are in emission. A further discussion of these lines is given in Sect. 3.

2.2. X-ray data and reduction

Gl 105B was observed with the ROSAT High Resolution Imager (HRI) from 5 August 1995 10:50 to 7 August 1995 07:54 giving a total effective integration time of 21373 sec. A detailed observing log is given in Table 2. The HRI is sensitive to photons in the energy range 0.1 – 2.1 keV. The effective area has three separate peaks, 0.28 keV, 0.5 keV and 1.1 keV, with the largest being at 1.1 keV. Its spatial resolution is 1.7 arc sec and field-of-view ∼18 arcmin. Reduction of the data was via the Starlink package, ASTERIX (Allan & Vallance 1995). The HRI image clearly shows the nearby K3 star, Gl 105A, but there is no obvious sign of Gl 105B. Careful reduction suggests an upper limit of 1 ± 5 10^{-4} $cts\,s^{-1}$ for Gl 105B. On-the-other-hand, Gl 105A is clearly detected at 16 ± 1 10^{-3} $cts\,s^{-1}$. Both of these objects are inactive stars and are expected to have coronal temperatures $< 10^6 K$ as opposed to the more active M dwarfs which have coronal temperatures of $\sim 10^7 K$ (e.g. see Schmitt et al., 1990). Using a Raymond-Smith model with $kT = 0.1\,keV$ and $N_H = 0$, we derive an observed flux at the Earth of 5.9 10^{-11} $erg\,cm^{-2}\,s^{-1}$ for Gl 105A or an X-ray luminosity of $logL_x = 27.53$. Given the above upper limits for Gl 105B, implies an X-ray flux at the Earth of $< 2.1\ 10^{-14}$ $erg\,cm^{-2}\,s^{-1}$ or an X-ray luminosity of $logL_x < 26.1$.

Table 2. ROSAT HRI observing run for Gl 105B

Date	Start UT	End UT
5 Aug 95	10:50:24	11:11:11
	14:02:01	14:19:56
	15:36:48	15:57:56
	18:51:43	19:16:19
	20:25:42	20:51:51
	23:35:41	00:03:00
6 Aug 95	05:48:17	08:00:50
	09:09:46	09:31:56
	13:55:55	14:12:56
	18:46:44	19:09:50
	20:18:52	20:45:26
	23:28:43	23:56:22
7 Aug 95	07:18:03	07:54:21

3. Chromospheric modelling

In a previous paper (Doyle et al. 1994), we discussed the observed Ca II HK fluxes for Gl 105B in terms of an inactive M dwarf. Here we use an updated set of calculations incorporating a subsample of four models from the grid presented by Andretta et al. (1997) and Short & Doyle (1997). This latter paper describes a method whereby background line opacity from 500 to 50000A is calculated using the model atmosphere code PHOENIX (Allard & Hauschildt 1995) with a resolution of $2A$ from the base of the photosphere to a point in the transition region with T = 20000 K. Fig. 1 shows the temperature structure of the models. The grid samples two values of the mass loading at the transition region, $m_{\rm o}$, and two values of the chromospheric temperature gradient, dT/d(logm) (or, equivalently, two values of the chromospheric thickness). As a result, the grid samples four values of $T_{\rm min}$. Following the model designations of Andretta et al. (1997), we denote the set of models of shallower and steeper dT/d(logm) as Series $1A$ and $2A$, respectively, see Fig. 1.

The cores of strong lines that form in the upper layers of the stellar atmosphere are affected by significant departures from Local Thermodynamic Equilibrium (LTE). Therefore, we must calculate the statistical equilibrium of the level populations and include the effect of scattering in the transfer of radiation. We have used the code MULTI (Carlsson 1986) to solve the combined radiative transfer and statistical equilibrium equations for

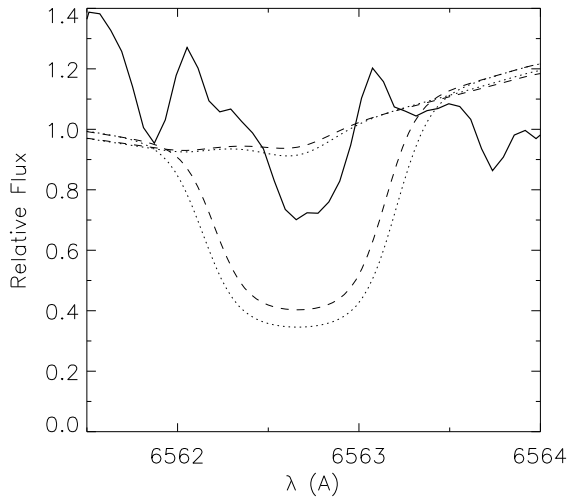

Fig. 2. Hα flux profile. Observed spectrum: solid line. Computed lines with models in series $1A$: dotted lines; $2A$ series: dashed lines. The lowest pressure models (lowest $m_{\rm o}$) are the ones that have the weakest line absorption.

atomic models of Hydrogen and Calcium. The Hydrogen model incorporates the lowest nine levels of H I and the H II state and the Calcium model incorporates eight levels of Ca I, five levels of Ca II, and the ground state of Ca III. Because the chromospheric $N_{\rm e}$ density structure is determined by the H I/H II ionization balance, we iterate the non-LTE solution of Hydrogen and the equation of hydrostatic equilibrium to convergence. The radiative transfer problem is solved in detail for all 36 $b-b$ transitions connecting the nine H I states and for the $b-f$ transitions of these states, and for ten $b-b$ and thirteen $b-f$ transitions in the Calcium atom. The atomic data for Calcium is from Drake (1991). The background line blanketing opacity was added to the continuous opacity normally computed by MULTI in the calculation of the background radiation field in the Lyα, Hα, and all nine $b-f$ transitions of Hydrogen, and for Ca I 4227, Ca II HK and all thirteen $b-f$ transitions of the Calcium atom. Short & Doyle (1997) and Short et al. (1997) have found that background line opacity can have a significant effect on the Hydrogen and Calcium spectra, and these papers contain a detailed analysis and discussion of this point.

The thick solid lines in Figs. 2 and 3 show the observed Hα and Ca II K line profiles. The background subtraction for the blue spectrum (Fig. 3) is estimated to be uncertain by $\pm$ 20%. Therefore, we have also plotted the observed spectrum with 20% of the mean flux added and subtracted to indicate the range of uncertainty in the flux level (thin solid lines). The observed Hα spectrum has not been rectified or flux calibrated. Therefore, because our synthetic spectrum is line blanketed, we have scaled the observed spectrum to force an overall match in the pseudo-continuum. The observed Ca II K spectrum has been flux calibrated, and has been scaled by a dilution factor of 1.0×10^{18} based on the distance and estimated radius of Gl 105B. The dashed lines show the computed profiles after degradation to the instrumental resolution by convolution with a Gaussian. The computed Ca II K profiles have been scaled by a factor of $B_\nu(T$ = 3200K$)/B_\nu(T$ = 3700K) (equal to 4.7) to compensate for the difference in $T_{\rm eff}$ between our model and an M3.5 star.

The Hα line is in absorption with moderate strength, which indicates intermediate activity level (dM). The computed $H\alpha$ profiles for the models of higher $m_{\rm o}$ value (dM models) are too strongly in absorption. On-the-other-hand, the dM(e) models produce a line profile which is much weaker than the observations indicate. This therefore indicates an atmosphere with $m_{\rm o}$ between -6.0 and -4.8. Although both dM models produce Hα profiles that are too wide, the series $2A$ model has a narrower profile and provides a closer fit than the series $1A$ model. In the case of Ca II K, the inner wings are too faint, particularly on the blue side, which may indicate an inaccuracy in the flux scaling due to an inaccuracy in the estimated value of either $T_{\rm eff}$ or the dilution factor. The dM models have emission cores that are somewhat stronger and wider than that of the observed profile, but which provide a much closer fit than the very weak emission cores of the dM(e) models. The emission core of the series $2A$ model provides a relatively good fit to the brightness and widths of the upper error limit of the observed profile. The predicted emission component of the series $1A$ model has a very pronounced central absorption component with widely separated emission peaks ($K2$ points) that are not seen in the observed spectrum. In contrast, the series $2A$ model has a less pronounced central self-absorption. The observed profile does not exhibit any central self-absorption. However, the resolution of the spectrum may be inadequate to reveal an absorption component as weak as that predicted by the series $2A$ model. The Ca II K profiles shown here were computed with the assumption of complete frequency redistribution (CRD) in the treatment of radiative transfer. The line core and inner wings are known to be partially coherent and this has a significant effect on the brightness and wavelength of the flux minima ($K1$ points) (Uitenbroek 1989). We are unable to calculate line profiles with partial frequent redistribution (PRD) with line blanketing in the background opacity. However, we have computed unblanketed PRD profiles for our models. For the intermediate activity models that provide the closest fit, PRD causes the emission core to brighten by $\approx$ 7% and has a negligible effect on the width of the emission core. The effect at the $K1$ points is larger, as expected. However, in this study we are only crudely assessing the activity level by a fit to the magnitude of the emission, and the effect of PRD on the emission strength is not large enough to affect our conclusions.

4. Discussion and conclusions

The Ca II HK surface flux is $\sim$ 6.5 10^3 $erg\ cm^{-2}\ s^{-1}$, which is only slightly less than the Mg II hk flux. Based on our chromospheric modelling, both the Hα and Ca II K line profiles indicate an intermediate activity dM chromosphere. Also, this modelling indicated that a better fit is obtained using a model atmosphere which has $T_{\rm min}$ less than 2650 K and a thin, steep chromosphere. Despite an effective integration time of

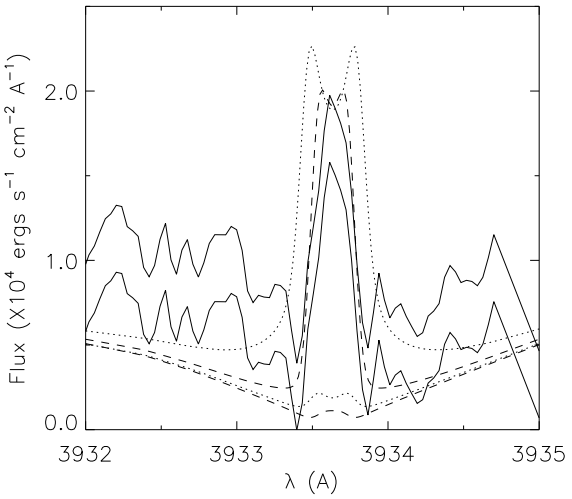

Fig. 3. Ca II K flux profile. Upper and lower uncertainty limits on observed spectrum: solid lines; Computed lines with models in series $1A$: dotted lines; $2A$ series: dashed lines. The lowest pressure models (lowest $m_{\rm o}$) are the ones that have the weakest central emission.

21,000 sec, Gl 105B was not detected in the X-rays implying $log\ L_x\ <\ 26.1$. Thus we are unable to draw any firm conclusions concerning the possibility of an acoustically heated corona as suggested by Mullan & Cheng (1994), although our observational data on GL 105B remain consistent with their suggestion.

Short & Doyle (1997) have shown that for the Hydrogen spectrum, contrary to previous expectations, excess emission in the *continuum*, rather than in the emission lines, dominates the radiative cooling of the chromosphere and lower transition region. For our best fit model to Gl 105B, we have computed the total excess emission in the continuum and in the Ca II HK line cores with respect to the lowest activity "basal" model in our grid. We find that the Ca II HK lines are responsible for only $\approx$ 5% of this total radiative loss. Therefore, we find that the Ca II spectrum, like the H I spectrum, is a minor coolant compared to the continuum in early M dwarfs.

Acknowledgements. We would like to thank the La Palma and ROSAT Observatory staff for their help in obtaining this data and in particular Drs. E. Zuiderwijk. Research at Armagh Observatory is grant-aided by the Dept. of Education for N. Ireland. We also acknowledge the support provided in terms of both software and hardware by the STARLINK Project which is funded by the UK PPARC. CIS is funded via a PPARC post-doctoral grant GR-H04613.

References

Allard, F., & Hauschildt, P. H., 1995, ApJ, 445, 433
Allan, D.J. & Vallance, R.J., 1995, *ASTERIX, Starlink User Note 98.6*
Andretta, V., Doyle, J. G., & Byrne, P. B., 1997, A&A, 322, 266
Byrne, P.B.: 1993b, A&A, 278, 520
Carlsson, M., 1986, Uppsala Observatory Internal Report no. 33
Doyle, J.G., Mathioudakis, M. Houdebine, E.R. & Panagi, P.M.: 1994, A&A 285, 233
Drake, J.J., 1991, MNRAS, 251, 369
Henry, T.S., Kirtpatrick, J.D. & Simons, D.A., 1994, AJ 108, 1437
Leggett, S.K., 1992, ApJ S 82, 351
Mathioudakis, M. & Doyle, J.G.: 1992 A&A 262, 523
Mullan, D.J. & Cheng, Q.-Q., 1994, ApJ 420, 392
Schmitt, J.H.M.M., Fleming, T.A. & Giampapa, M.S., 1995, ApJ 450, 392
Schmitt, J.H.M.M., Collura, A., Sciortino, S., Vaiana, G.S., Harnden, F.R. & Rosner, R., 1990, ApJ 365, 704
Short, C. I. & Doyle, J. G., 1997, A&A, in press
Short, C. I., Doyle, J. G., & Byrne, P. B., 1997, A&A, in press
Stauffer, J.R. & Hartmann, L.W., 1986, ApJS 61, 531
Uitenbroek, H., 1989, A&A 213, 360
Ulmschneider, P.: 1991, 'Mechanisms of Chromospheric and Coronal Heating, eds. P. Ulmschneider et al. (Berlin: Springer-Verlag), p328
Unger S., Pettini M. *UES User's Manual. Isaac Newton Group, La Palma, 1993*

This article was processed by the author using Springer-Verlag LaTeX A&A style file *L-AA* version 3.